Analysis of Trends in TF vs. Angle and Depth

It is assumed that kerma decreases with depth in the measured material after electron equilibrium is reached, as discussed in Chapter 7, Part A. The Hiroshima TF values in Tables 2 and 3 are plotted in Figure 8 vs. the inverse of the cosine of angle of incidence for various intervals of mean mass thickness depth, where the mean mass thickness depth is obtained by taking the depth (perpendicular to the surface) in cm to the middle of the measured material and multiplying it by the density noted for that sample in Appendix 11. (The mass thickness depth at a linear depth d perpendicular to the surface is therefore the mass of material per unit cross-sectional area (per cm^2) from the surface to that depth.) This method of depicting the data in a two-dimensional plot, as opposed to classifying the data into a few intervals of angle and plotting the data in each interval as a series vs. mass thickness depth, was chosen initially because the samples as characterized by Kaul et al. (1987) had a few, common density values and were measured at a few, common ranges of depth.

A feature that is immediately apparent is that the TFs calculated for measurements at mass thickness depths in the range from 2.7 to 3.4 g/cm^2 in Hiroshima (filled blue circles) lie on a smooth curve. Although not as visually apparent, and confined to smaller angles, the data in the same mass thickness interval for Nagasaki (open blue circles) also fall near a single curve, but at a different level. With the exception of one *datum* in Nagasaki, these are all JNIRS 1967 measurements (Hashizume et al. 1967), as shown by the open red circles and squares. All but one

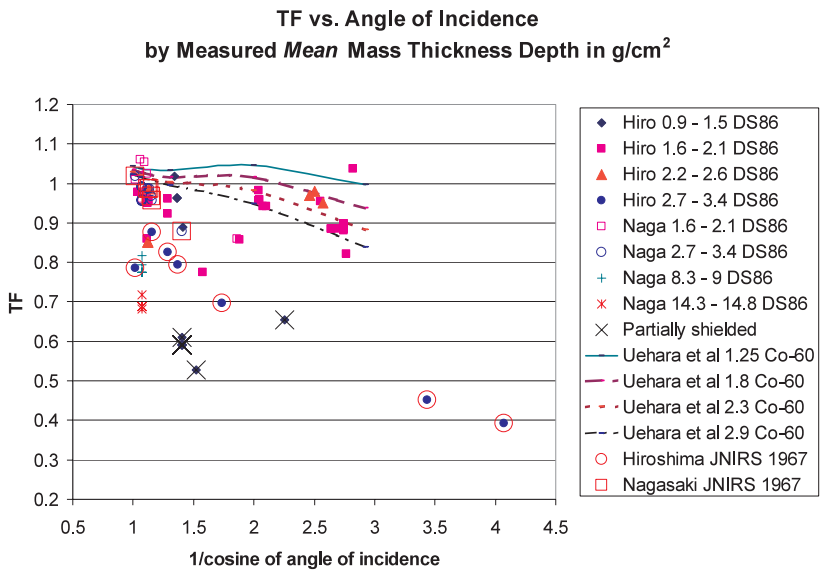

Figure 8. *Transmission factor vs. 1/cosine of the angle of incidence, subclassified by the arithmentic mean of the depth of the measured material in units of mass thickness, i.e., g/cm^2, for Hiroshima and Nagasaki. The calculated values of Uehara et al. (1988) for a monodirectional beam of ^{60}Co gamma rays, converted from depth dose to the type of TF shown here, are plotted for comparison.*

of the samples of this set in each city are wall tile samples. These wall tile samples, in addition to being measured at the same depths and being calculated based on the same density, were modeled for the Monte Carlo calculations of Kaul et al. by using the same, identical, simplified building model: a simple rectangular box, with the sample located in an identical position on a building of identical size. The curves for the Hiroshima and Nagasaki TFs appear almost parallel but with Hiroshima being almost 0.1 less than Nagasaki at the same mass thickness depths. As these particular samples were modeled with the measured volume at the same perpendicular mass thickness depth (2.0 g/cm^3 density, between 1 and 2 cm deep), it appears that the Nagasaki gamma fluence was more penetrating than the Hiroshima gamma fluence. More generally and more importantly, the calculations within each of these two sets differ only in two respects: distance-specific incident gamma and neutron fluences, and angles of incidence. The angles of incidence, which are equal to the angles of elevation because all are vertical samples at perpendicular azimuthal angles, form a neat progression that depends on modeled ground distance as the arctangent of the height of burst divided by ground distance. Thus these values show the effect of depth as determined by angle of incidence with all other factors held constant.

The leftmost JNIRS 1967 TF in each city is for a sample that was modeled as a roof tile. Although the roof tile value for Nagasaki falls neatly on a curve with the wall tile samples, the value in Hiroshima is unexpectedly low. Another feature depicted is that the samples explicitly noted by Kaul et al. as being partially shielded—all samples at the Chugoku Electric Co. and one of two samples at the Postal Savings Bureau—are denoted by additional collocated symbols "X."

In addition, values calculated by Uehara et al. (1988) have been converted from depth dose as defined by them to the type of TF depicted here, and plotted for comparison. We took values from their Figure 7 for ^{60}Co, in which they plotted depth dose as cGy to tile per R of exposure in the unattenuated beam (1 R = 0.258 mC/kg in air). Dose to quartz is presumed equal to dose to tile in both their calculation and DS86, and Uehara et al. obtained a conversion of 0.865 cGy/R for tile free in air by taking 0.869 times the ratio of mass energy absorption coefficients for tile and air for ^{60}Co gammas. Therefore, as they were plotting Gy to quartz at depth per 0.865 Gy to quartz FIA, we divided their plotted values by 0.865 to get values equivalent to the "Type 1 TF" calculated in this work, which latter is Gy to quartz *in situ* per Gy to quartz FIA at the same exact location, with no correction for sample elevation and no building gammas involved. We took their values, which are plotted as depth dose at 2-mm intervals of linear depth for the previously noted discrete angles, and performed a lowess (moving average) smooth on the data for each angle to remove small oscillations in the plotted step functions vs. depth. We took their stated depths in cm, multiplied them by their assumed density of 1.786 g/cm^3 to get mass thickness depths, and selected appropriate values from the results, interpolating them if necessary to get values corresponding roughly to the midpoints of the mass thickness intervals used in our plot. Finally, we added these to our plot and put smoothed lines through them.

Of course, the values of Uehara et al. are not directly comparable to those calculated for DS86, for several reasons: the former were for monodirectional beams of gamma rays at two discrete energies, whereas the latter are highly polydirectional and polyenergetic, the former were calculated for a very idealized sample geometry with a localized beam, whereas the latter were calculated for a fluence at all angles incident on a larger structure containing the sample, and the assumed elemental compositions were similar but not identical. Nevertheless, the curves from the data of Uehara et al. give some idea what to expect in terms of general trends. Unfortunately, the DS86 data are sparse, unevenly distributed, and very noisy due to the effects of the modeled

structures, for all mass thickness categories except the one just described as pertaining to the JNIRS 1967 measurements, and it is very difficult to discern trends.

Because examination of several individual cases indicated that the minimum measured mass thickness depth might contain more information than the mean measured mass thickness depth, the type of plot shown in Figure 9 was examined. The data do appear to be more ordered with respect to depth in this plot, although still very noisy and overlapping. The data from Uehara et al. (1988) shown in this plot have been re-selected to correspond roughly to the intervals of minimum rather than mean mass thickness used for the DS86 calculations. A notable feature in this regard is that the data of Uehara et al. for the first two or three mass thickness depths shown, especially the curve for 0.36 g/cm^2, are actually lower at acute angles of incidence (left side of plot), presumably because such shallow depths are in the area of electron disequilibrium ("buildup layer"). However, we should not expect to see much of this effect in even the shallowest measured samples calculated for DS86, as their measured volumes are considerably thicker than the 2-mm layers of Uehara et al.

An additional feature shown in this plot is that simple exponentials have been fitted to the JNIRS 1967 wall tile data, i.e., a simple linear regression of the logarithm of the TF on the inverse of the cosine was performed. The excellent fit that can be obtained with a simple exponential suggests that attentuation is close to being an exponential function of the angled depth d_{ang} when density is held constant, independent of distance from the hypocenter (i.e., no major trend due to distance-dependent changes in incident fluence spectrum). This is a very important point, which is used in this work, as described below, both to adjust the JNIRS 1967 TFs for new information that affects the angle of incidence, and to devise a method for estimating TFs for structures not calculated in DS86. In the Hiroshima case, the data were fitted both with and without the two low values at the most oblique angles; the latter case is shown here. Since a more obtuse angle is effectively a greater mass thickness depth, the general trend seen here suggests that there is some minor beam hardening with depth, so that TFs do not fall off quite as rapidly at deeper depths as at depths just beyond the point of electron equilibrium.

Because it would be difficult to fit a family of curves to the data in Figures 8 and 9, and even more difficult to use them to estimate a TF for some new set of input parameters, we sought a way to use the physics of radiation attenuation to combine density, depth, and angle into a single useful parameter that could be used to estimate the TF. An obvious choice was to take the minimum (or perhaps mean) mass thickness depth and divide it by the cosine of the angle of incidence, giving a mass thickness depth corresponding to the linear thickness of material that an incident ray would traverse to reach a perpendicular depth d. We refer to this here as an "angled mass thickness depth," i.e., the mass thickness associated with the thickness d_{ang} in Figure 3. This is really just a matter of adjusting the angled depth d_{ang} for density. Although we noted above that the trend in the JNIRS 1967 measurements suggests that attenuation is indeed an exponential function of the angled depth, and the density adjustment is a simple extension, the problem in extending this to calculating new TFs is that there is a substantial thickness of measured material involved. In the JNIRS 1967 measurements, every sample was calculated with a measured depth from 1 to 2 cm, and a unit perturbation in the angle of incidence affects the angled depth to every perpendicular depth in equal proportion, viz., $d_{ang} = d / \cos \tau$ for all d. However, this is not true among the other samples with their varying depths and thicknesses of measured material. To obtain a metric that might summarize the effect of a given range of measured depths in a useful way, we tried two possibilities. One was the angled mass thickness depth to the minimum

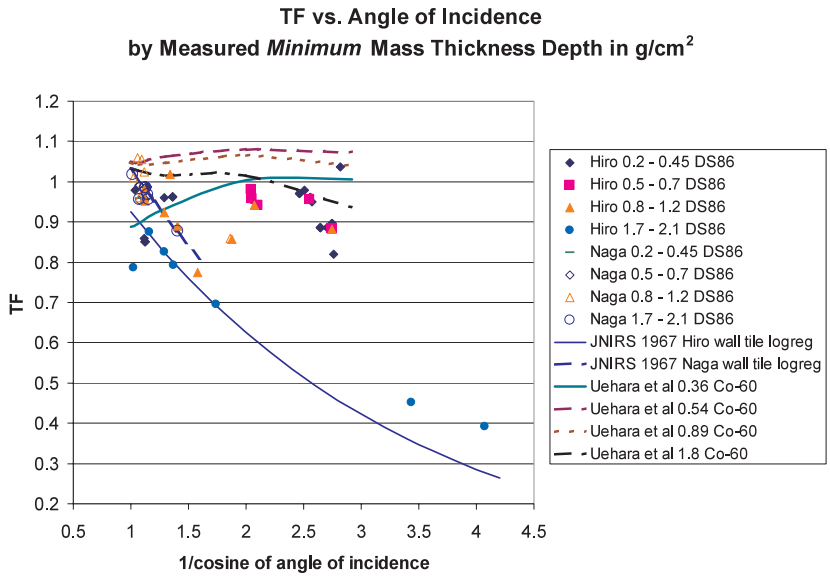

Figure 9. *Transmission factor vs. 1/cosine of the angle of incidence, subclassified by the minimum depth of the measured material in units of mass thickness, i.e., g/cm^2, for Hiroshima and Nagasaki. The calculated values of Uehara et al. (1988) for a monodirectional beam of ^{60}Co gamma rays, converted from depth dose to the type of TF shown here, are plotted for comparison.*

measured depth, based on the previous discussion of Figures 8 and 9. The other was the geometric mean angled mass thickness depth, based on the idea that attenuation is exponential rather than linear. The first is shown in Figure 10 and the second in Figure 11. The curves labelled "logreg" are simply linear regressions on the logarithms of the specified data.

We omitted the DS86 result for the "house at Nobori machi" from the plots in Figures 10 and 11 and the related regressions, because a credible azimuthal angle could not be estimated. The value given in Figure 6 of Kaul et al. (1987), 180° does not seem plausible, and the angle estimated with the GIS was uncertain due to the inability to clearly identify the house on an aerial photograph, and led to an anomalous result. In addition, we omitted those samples explicitly noted as being partially shielded by Kaul et al. (all samples at the Chugoku Electric Co., a wall tile sample RERF List No. 6-04 at the Postal Savings Building). However, we retained other samples with more subtle indications of probable partial frontal shielding, such as the tiles RERF List No.'s 3-16 and 3-17 on the roof of the Hiroshima University Faculty of Science ("E") Building, in the dataset. We did not use the univariate regressions shown in Figures 10 and 11 to estimate TFs for this work, because a better, multivariate "loglinear" model was developed as discussed below.

When duplicate calculations of the same sample were omitted, there were 42 total observations in Hiroshima, of which 22 were horizontal tiles and 20 were vertical. (For the purposes of this particular analysis, slanted tiles were considered horizontal, since they were tilted only slightly from the horizontal.) There were 28 observations in Nagasaki, of which only

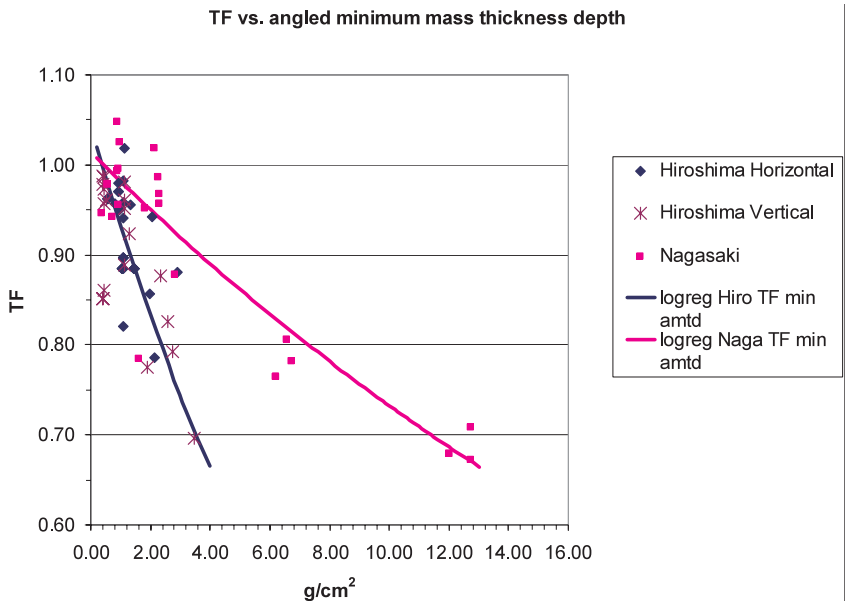

Figure 10. *Transmission factor vs .the angled minimum mass thickness depth, defined as the inverse of the cosine of the angle of incidence times the minimum depth of the measured material in units of mass thickness, i.e., g/cm^2, for Hiroshima and Nagasaki.*

one was horizontal. Because Kaul et al. observed that the horizontal and vertical tiles were somewhat different, we included this aspect in the analysis. In Hiroshima, the horizontal tiles had a mean TF of 0.92 vs. 0.85 for vertical tiles. The vertical tiles in Nagasaki had a mean TF of 0.89. When a Wilcoxon rank-sum (Mann-Whitney) nonparametric test was done to test the equality of distribution among the horizontal vs. vertical tiles in Hiroshima, the result was not close to significance (no significant difference). However, the term for "horizontal vs. vertical" *was* significant in the multivariate model discussed below. Statistically, the reason for this is that the latter analysis has more power to detect an effect of horizontal vs. vertical orientation, but its results are subject to the more specific assumptions of the multivariate loglinear model.

To produce a better model for fitting the data, we decided to put all of the candidate measures of angled mass thickness depth, along with a dummy variable for horizontal vs. vertical orientation, into a multivariate model, and select the best predictors by a standard hierarchical model selection process that begins with the full model and successively eliminates statistically insignificant variables. When we did this for Hiroshima using multiple linear regression of log TF on the minimum, geometric mean, and maximum angled mass thickness depth, along with a dummy variable for horizontal vs. vertical, (i.e., a "log-linear model" In(TF) = $\beta_0 + \beta_1 X_1 + \beta_2 X_2 + \ldots + \beta_k X_k + \varepsilon$ in which the X-variables are the angled mass thickness depth variables or a dummy variable for horizontal vs. vertical, and ε is an error term), the best model was minimum and maximum angled mass thickness depth plus horizontal-vertical, with all terms highly signficant. Of course, as geometric mean angled mass thickness depth is a function of minimum

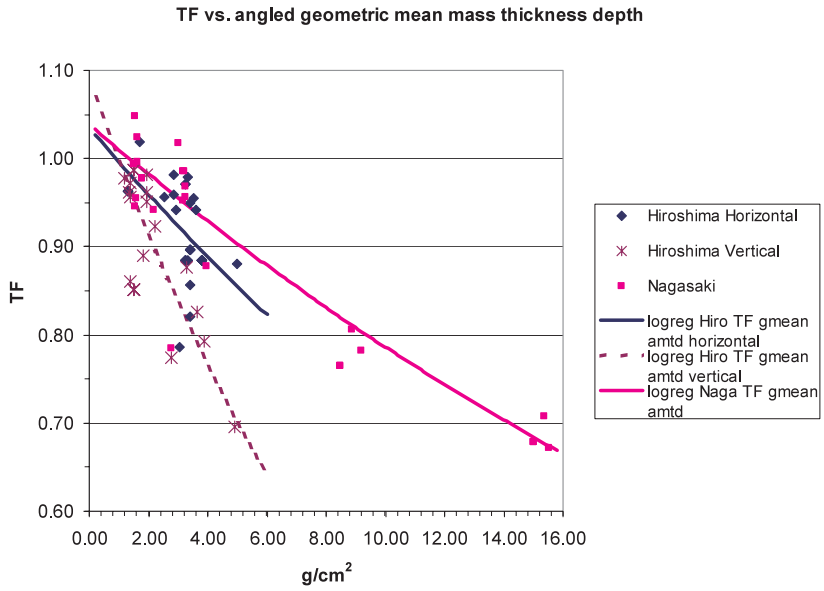

Figure 11. *Transmission factor vs. the angled geometric mean mass thickness depth, defined as the inverse of the cosine of the angle of incidence times the geometric mean of the depth of the measured material in units of mass thickness, i.e., g/cm^2, for Hiroshima and Nagasaki.*

and maximum angled mass thickness depth (the square root of their product), one does not anticipate that all three would be significant terms in the regression. When models were tested for Nagasaki using multiple linear regression of log TF on the minimum, geometric mean, and maximum angled mass thickness depth, the best model was minimum and geometric mean angled mass thickness depth, again with all terms highly signficant. These models, with the fitted coefficients shown in Table 4a, were used to estimate the Type 1 TF without building gammas for samples not calculated in DS86. To show how the model performs in estimating the TF we give the residuals from the regression, shown as the ratio of each regression estimate to the actual TF calculated by Kaul et al. in Table 4b.

Table 4a. Fitted regression coefficients for estimating logarithm of Type 1 TF

	Hiroshima	Nagasaki
Intercept	0.1310155	0.0995873
Minimum amtd[a]	-0.095655	0.0902555
Geometric mean amtd[a]	0	-0.104212
Maximum amtd[a]	-0.011206	0
Horizontal/vertical[b]	-0.075565	0

[a]amtd = angled mass thickness depth in g/cm^2.
[b]Horizontal/vertical = 0 if sample is horizontal, 1 if vertical.

Table 4b. Loglinear model results for estimating Type 1 TF

City	Place	Sample ID#	RERF list No.	DS86 TF	TF estimated by loglinear regression model	Ratio of regression estimate to DS86 TF
H	A-bomb Dome			0.786	0.885	1.126
H	Togiya-cho Shojun-ji			0.392	0.405	1.033
H	Nenryo Kaikan (Fuel Authority Bldg)			0.451	0.470	1.042
H	Fukuro-machi East Orthopedic Surgical Hospital			0.696	0.701	1.007
H	Naka Telephone Office	3	1-1	1.019	0.994	0.975
H	Naka Telephone Office	2	1-19	0.774	0.841	1.087
H	Naka Telephone Office	203-3	1-4	0.962	1.044	1.085
H	Tate-machi Sanin Godo Bank			0.793	0.764	0.963
H	Sanin Bank		12-2	0.889	0.917	1.031
H	Nobori-machi Elementary School			0.825	0.779	0.944
H	City Hall			0.876	0.803	0.917
H	H.U.P.S. (Hiro. Uriv.)	H-1	4-08	0.970	0.922	0.951
H	H.U.P.S. (Hiro. Univ.)	H-2	4-07	0.987	0.957	0.970
H	H.U.P.S. (Hiro. Univ.)	H-3	4-09	0.979	0.919	0.939
H	H.U.P.S. (Hiro. Univ.)	H-4	4-01	0.987	0.958	0.971
H	H.U.P.S. (Hiro. Univ.)	H-5	4-03 horizontal	0.950	0.914	0.962
H	H.U.P.S. (Hiro. Univ.)	H-5B	4-03 vertical	0.852	0.958	1.124
H	H.U.F.S. (Hiro. Univ.)	7	3-07	0.981	0.915	0.933
H	H.U.F.S. (Hiro. Univ.)	HPl	3-08	0.972	0.966	0.994
H	H.U.F.S. (Hiro. Univ.)	10	3-10	0.951	0.913	0.960
H	H.U.F.S. (Hiro. Univ.)	H-6-1	3-20	0.885	0.924	1.044
H	H.U.F.S. (Hiro. Univ.)	HP2	3-11	0.957	0.966	1.009
H	H.U.F.S. (Hiro. Univ.)	UHFSO3	3-23	0.982	0.948	0.965
H	H.U.F.S. (Hiro. Univ.)	H-7	3-36	0.957	0.969	1.013
H	H.U.F.S. (Hiro. Univ.)	UHFSO2	3-22	0.959	0.948	0.989
H	H.U.F.S. (Hiro. Univ.)	H-8	3-18	0.885	0.920	1.040
H	H.U.F.S. (Hiro. Univ.)	I	3-29	0.961	0.914	0.951
H	H.U.F.S. (Hiro. Univ.)	IV	3-31	0.942	0.873	0.927
H	H.U.F.S. (Hiro. Univ.)	H- 9	3-17	0.860	0.966	1.123
H	Red Cross Hospital		5-01	0.923	0.894	0.969
H	Red Cross Hospital	HP4	5-01	0.961	0.966	1.005
H	H.U.F.S. (Hiro. Univ.)	R1	3-35	0.881	0.787	0.893
H	H.U.F.S. (Hiro. Univ.)	UHFSFT02	3-35	0.885	0.890	1.006
H	H.U.F.S. (Hiro. Univ.)	H-10-1	3-15	0.897	0.917	1.022
H	H.U.F.S. (Hiro. Univ.)	UHFS04	3-24	0.955	0.906	0.949
H	H.U.F.S. (Hiro. Univ.)	UHFS07	3-27	0.942	0.943	1.001
H	H.U.F.S. (Hiro. Univ.)	H-11	3-16	0.821	0.916	1.116
H	Chokin-Kyoku		6-00	0.857	0.884	1.032
H	HUFE	HP5	8-01	0.978	0.978	1.000

Table 4b. Continued

City	Place	Sample ID#	RERF list No.	DS86 TF	TF estimated by loglinear regression model	Ratio of regression estimate to DS86 TF
N	Yamazoto-cho House			1.018	0.978	0.961
N	Urakami		N4	0.860	0.958	1.114
N	Urakami Church			0.878	0.941	1.072
N	Hachiman jinja nearby house			0.957	0.968	1.012
N	Hachiman jinja			0.968	0.969	1.001
N	Sakamoto cho Gaijin Cemetery			0.986	0.970	0.984
N	Sakamoto-cho Gaijin Cemetery			0.986	0.972	0.985
N	Sakamoto		N-6	1.055	1.016	0.963
N	Ieno wall	NAIEO5	N-2-1	0.992	0.964	0.971
N	Ieno wall	NAIEO5	N-2-1	0.775	0.797	1.029
N	Ieno wall	NAIEO5	N-2-1	0.688	0.684	0.994
N	Ieno wall	NAIEO5	N-2-1	0.992	0.964	0.971
N	Ieno wall	NAIEO5	N-2-1	0.775	0.797	1.029
N	Ieno wall	NAIEO5	N-2-1	0.688	0.684	0.994
N	Ieno	A	N-2-2	0.961	1.018	1.059
N	Ieno	B	N-2-2	0.957	0.937	0.980
N	Ieno wall	A	N-2-1	0.959	0.972	1.013
N	Ieno wall	B	N-2-1	0.817	0.792	0.969
N	Ieno wall	C	N-2-1	0.682	0.692	1.014
N	Ieno wall	NAIEO5	N-2-1	0.992	0.964	0.971
N	Ieno wall	NAIEO5	N-2-1	0.775	0.797	1.029
N	Ieno wall	NAIEO5	N-2-1	0.688	0.684	0.994
N	Ieno wall	NAIEO6	N-2-1	0.955	0.940	0.984
N	Ieno wall	NAIEO6	N-2-1	0.793	0.778	0.981
N	Ieno wall	NAIEO6	N-2-1	0.718	0.702	0.978
N	Zenza		N-7	1.060	1.019	0.961
N	Inasa	A	N-3	1.025	1.014	0.989
N	Chikugo		N-8	1.009	1.021	1.012

The results for Hiroshima are reasonable from first principles, in that we would expect the overall TF to decrease with increase in both minimum and maximum measured depth, although the reason for the difference between horizontal and vertical samples is not immediately apparent, and presumably relates to the angle-energy distribution of the incident fluences. The result for Nagasaki seems odd in that the sign of the coefficient for minimum angled mass thickness depth is not negative. This may be a result of attempting to fit values that were calculated for a set containing a mixture of 1) relatively shallow and thin measured depths along with 2) much deeper and thicker measured depths at the Ieno wall.

Rule for Determining DS02 TFs

For samples calculated in DS86, the DS86 TFs without the building gamma component as shown in Tables 2 and 3 were used unchanged for this work, and the building gamma component was calculated as described below. Some cases of post-DS86 measurements (and two cases of the 1967 Hashizume measurements as discussed in the next paragraph) were suitable for direct application of the DS86 TFs. These are cases in which samples were measured after DS86 from the same exact location as one that was modeled in Appendix 11, or samples were measured from a DS86 location with identical sample-structure geometry.

One improvement on the information that was available for Appendix 11 was to allow more specific TFs to be used for two of the Hashizume 1967 samples. These samples were identified with information about their specific location in an internal RERF report by H. Yamada, dated November 18, 1981, which was translated from the Japanese and used in the determinations of map coordinates for this work, and provided the information in the "place and sample" column of Tables 2 and 3 for those samples (footnote a to the table). Thus, it seemed logical that the more specific TFs calculated for the same location for a sample measured for DS86 could be used in place of the generic calculation in cases where a 1967 sample was from the same building and same geometry as a DS86 sample (San'in Godoh Bank, Urakami Church). However, because the JNIRS 1967 samples were measured at a considerably deeper depth (1-2 cm vs. 0.5-1.5 cm) than the samples measured later and calculated for DS86 at the same locations, we decided instead to use the adjustment method described below for the JNIRS 1967 samples on these as on the others in that set. That is, we used a regression of TF on the inverse of the cosine of the angle of incidence to correct for a different angle of incidence assumed in this work than that used by Kaul et al., which is equivalent to sliding the TFs along the curves illustrated in Figure 9.

For samples not calculated in DS86, we estimated the TF using the log-linear equation described above with the coefficients given in Table 4.

For the NUE 1966 measurements in Hiroshima (Ichikawa et al. 1966), we assumed an azimuthal angle of 45°, based on a uniform distribution from 0° to 90°. Because these samples were collected from roof tiles that had fallen during the blast in most cases, it seems unlikely that they were on a roof surface with any azimuthal orientation more specific than being within a half-circle centered on the direction to the hypocenter. Furthermore, it was not possible to identify structures whose azimuthal angle could be estimated using the GIS. If the azimuthal orientation of the tile is uniformly distributed on the half circle from 0° to 180°, then the smaller of two complementary azimuthal angles between the surface (or its tilt axis) and a ray to the hypocenter (as defined above in the discussion of Figure 4) is uniformly distributed on the interval from 0° to 90°. Based on photographs of temple roofs, which are curved and range from near-horizontal slant angles at the edge to near-vertical slant angles at the center, we also assumed a slant angle of 45°. Therefore we assigned a value of 0.5 for the horizontal-vertical dummy variable for these samples.

We gave the JNIRS 1967 samples revised TFs calculated with a new angle of incidence based on the DS02 GR, a GIS-evaluated DS02 ground elevation (for Nagasaki samples only), and a GIS-evaluated DS02 azimuthal angle. For the Nagasaki samples, because the azimuthal angle could not be estimated using the GIS, due to the inability to see the particular structures involved, we used the average azimuthal angle estimated with the GIS for the JNIRS samples in Hiroshima, which equated to a 15° azimuthal deflection from the perpendicular. For the vertical wall tile

JNIRS 1967 samples and only for those samples we used the simple regression of log TF on the inverse of the cosine of the angle of incidence, rather than the full log-linear models involving angled mass-thickness depth and horizontal vs. vertical orientation. We chose this approach because all of the parameters other than angle of incidence were identical among the vertical JNIRS 1967 samples as modeled by Kaul et al., and because we could apply a regression based on the results of Kaul et al. for a single adjoint Monte Carlo model designed specifically for these samples, rather than a regression based on their results for a group of adjoint Monte Carlo models of various structure-sample geometries. All samples in Hiroshima except the two most oblique in Hiroshima were estimated with an intercept of 1.37 at zero depth and a relaxation length of 5.10 cm; the latter were estimated with an intercept of 1.16 at zero depth and a relaxation length of 7.38 cm. All samples in Nagasaki were estimated with an intercept of 1.54 at zero depth and a relaxation length of 4.99 cm.

For samples calculated in DS86, we estimated the DS02 building gamma component by correcting for differences in neutron fluence using a ratio of ^{60}Co activation for DS02 to that for DS86, and we corrected for the DS02 slant range using the inverse square of distance and an exponential with the relaxation lengths described above and corresponding to the solid lines in Figures 1 and 2. For samples not calculated in DS86, we simply used the exponential model from the regression described above and corresponding to the solid lines in Figures 1 and 2, with the DS02 slant range, multiplied by the DS02-DS86 ^{60}Co activation ratio at that distance.

In summary, using the values from Appendix 11 to Chapter 4 of the DS86 Final Report, with the same designations of prompt primary, delayed, and other components used here as subscripts, we defined

$$TF_{DS86\_with\_Bldg\_gamma} \equiv$$

$$\frac{D_{DS86\_in\_situ\_calc_{P+S}}(SR(GR_{86},ht_{86},elev_{86})) + D_{DS86\_in-situ\_calc_{DG}}(SR(GR_{86},ht_{86},elev_{86}))}{D_{DS86\_FIA\_calc_{P+S}}(SR(GR_{86},ht_{86},elev_{86})) + D_{DS86\_FIA\_calc_{DG}}(SR(GR_{86},ht_{86},elev_{86}))} +$$

$$\frac{D_{DS86\_in\_situ\_calc_{BG\_P}}(SR(GR_{86},ht_{86},elev_{86})) + D_{DS86\_in-situ\_calc_{BG\_D}}(SR(GR_{86},ht_{86},elev_{86}))}{D_{DS86\_FIA\_calc_{P+S}}(SR(GR_{86},ht_{86},elev_{86})) + D_{DS86\_FIA\_calc_{DG}}(SR(GR_{86},ht_{86},elev_{86}))} \quad (5)$$

$$TF_{DS86\_without\_Bldg\_gamma} \equiv$$

$$\frac{D_{DS86\_in\_situ\_calc_{P+S}}(SR(GR_{86},ht_{86},elev_{86})) + D_{DS86\_in-situ\_calc_{DG}}(SR(GR_{86},ht_{86},elev_{86}))}{D_{DS86\_FIA\_calc_{P+S}}(SR(GR_{86},ht_{86},elev_{86})) + D_{DS86\_FIA\_calc_{DG}}(SR(GR_{86},ht_{86},elev_{86}))} \quad (6)$$

To obtain DS02 calculated *in situ* doses for samples calculated in DS86, we used the DS86 TF without building gammas times the DS02 calculated FIA kerma, plus a separately calculated building gamma component that we obtain by taking the DS86 building gamma component and adjusting for thermal neutron fluence ratios and slant range differences:

$$D_{DS02\_in\_situ\_calc} \equiv$$

$$\{ TF_{DS86\_without\_Bldg\_gamma} \times [D_{DS02\_FIA\_calc_{P+S}}(SR(GR_{02}, ht_{02}, elev_{02})) +$$

$$D_{DS02\_FIA\_calc_{DG}}(SR(GR_{02}, ht_{02}, elev_{02}))] \}$$

$$+ \{ [D_{DS86\_in\_situ\_calc_{BG\_P}}(SR(GR_{86}, ht_{86}, elev_{86})) + D_{DS86\_in-situ\_calc_{BG\_D}}(SR(GR_{86}, ht_{86}, elev_{86}))] \times$$

$$\frac{^{60}Co\_activ_{DS02}(GR_{02})}{^{60}Co\_activ_{DS86}(GR_{02})} \times \frac{(SR(GR_{02}, ht_{02}, elev_{02}))^2}{(SR(GR_{86}, ht_{86}, elev_{86}))^2} \times$$

$$\exp[(SR(GR_{86}, ht_{86}, elev_{86}) - SR(GR_{02}, ht_{02}, elev_{02}))/ RL_{Bldg\_gamma_{DS86}}] \} \quad (7)$$

where RL is the city-specific relaxation length described above for DS86 building gammas. That is, for any sample calculated in DS86 except for the JNIRS 1967 measurements, we defined

$$TF_{DS02\_without\_Bldg\_gamma} \equiv TF_{DS86\_without\_Bldg\_gamma} \quad (8)$$

applied that TF to the DS02 free-in-air kerma at the appropriate DS02 slant range for that sample, and added the building gamma component corrected as shown for the difference between DS86 and DS02 slant range.

For the JNIRS 1967 measurements, we adjusted the DS86 TF for a new angle of incidence τ_{DS02} based on the DS02 GR, DS02 sample elevation, and a GIS-estimated azimuthal deflection φ_{DS02} not assumed = 0^o as in DS86. This adjustment is based on a regression of log TF on $1/\cos\tau_{DS86}$ for the DS86 TFs of the JNIRS 1967 measurements. That is,

$$TF_{DS02\_without\_Bldg\_gamma} = ae^{\frac{b}{\cos\tau_{DS02}}} \quad (9)$$

where a and b are coefficients determined by the regression

$$\ln(TF_{DS86\_without\_Bldg\_gamma}) = \alpha + \beta\frac{1}{\cos\tau_{DS86}} + \varepsilon \quad (10)$$

on an appropriate subset of the JNIRS 1967 measurements, i.e., $a = e^{\hat{\alpha}}$, $b = \hat{\beta} = \frac{1}{RL}$, where the intercepts a and the RL's are those given above.

For samples not calculated in DS86, in Hiroshima, we estimated $TF_{DS02\_without\_Bldg\_gamma} = ae^{bmin\_amtd+cmax\_amtd+dhor\_vert}$ where ln(a), b, c, and d are the coefficients given in Table 4, and in Nagasaki we estimated $TF_{DS02\_without\_Bldg\_gamma} = ae^{bmin\_amtd+cgeom\_mean\_amtd}$ where ln(a), b, c, and d are the coefficients given in Table 4.

We then estimated

$$D_{DS02\_in\_situ\_calc} = \{ TF_{DS02\_without\_Bldg\_gamma} \times [D_{DS02\_FIA\_calc_{P+S}}(SR(GR_{02}, ht_{02}, elev_{02})) +$$

$$D_{DS02\_FIA\_calc_{DG}}(SR(GR_{02}, ht_{02}, elev_{02}))] \}$$

$$+ [\exp(BG_0 - \frac{SR(GR_{02}, ht_{02}, elev_{02})}{RL_{Bldg\_gamma_{DS02}}}] \times \frac{^{60}Co\_activ_{DS02}(GR_{02})}{^{60}Co\_activ_{DS86}(GR_{02})} \quad (11)$$

with BG_0 being the intercept and $RL_{Bldg\_gamma_{DS02}}$ the inverse of the slope of the regression of the logarithm of the building gamma component on slant range, i.e., the values of dose and relaxation length documented above in the section “Calculation of DS02 Building Gamma Kerma” and illustrated by the regression lines in Figures 1 and 2.

Tables 5 and 6 show the samples for which TFs were estimated using the loglinear model, including the adjusted estimates of the TFs for the JNIRS 1967 samples, and give the input data along with the TF with and without the calculated building gamma component. Tables 7 and 8 show the DS86 samples except for the JNIRS 1967 samples, and the samples for which we adopted corresponding TFs calculated in DS86, indicating for the latter which TF was adopted and giving the TFs with and without the DS02 building gamma component. (The TF without the DS02 building gamma component is the DS86 TF.)

Table 5. DS02 Type 1 TFs estimated or adjusted based on analysis of DS86 TFs: Hiroshima

Lab	Place name	Sample ID#	RERF list No.	DS02 GR (m)	DS02 ht (m)	Elevation angle (deg)	Azimuthal angle (deg)	Angle of incidence (deg)	Meas. depth (cm)	Density (g/cm^3)	TF, no bldg gamma	TF with bldg gamma
JNIRS	Togiya-cho Shojun-ji			337	3	60.6	77.7	61.3	1-2	2	0.659	0.818
JNIRS	Nenryo Kaikan (Fuel Authority Bldg)			158	3	75.2	78.9	75.5	1-2	2	0.393	0.573
NUE	Zaimoku cho, Dempuku ji	H-1		410	4	55.5	45	30.0	2.2-3.9	2.1	0.593	0.696
NUE	Zaimoku cho, Seigan ji	H-2		401	4	56.1	45	30.0	2.2-3.9	2.1	0.593	0.698
NUE	Zaimoku cho, Seigan ji	H-2'		401	4	56.1	45	30.0	2.2-3.9	2.1	0.593	0.698
JNIRS	Fukuro-machi East Orthopedic Surgical Hospital			421	3	54.8	69.4	57.4	1-2	2	0.662	0.790
NUE	Zaimoku cho,	H-3		424	4	54.6	45	30.0	2.2-3.9	2.1	0.593	0.694
JNIRS	Tate-machi Sanin Godo Bank			624	3	43.0	74.0	45.9	1-2	2	0.780	0.859
JNIRS	Nobori-machi Elementary School			716	3	39.8	76.3	41.7	1-2	2	0.810	0.872
NUE	Hiroshima Castle, ninomaru	H-4		739	4	38.9	45	33.6	0.2-1.9	2.1	0.991	1.048
NUE	Hiroshima Castle, ninomaru	H-4'		739	4	38.9	45	33.6	0.2-1.9	2.1	0.991	1.048
NUE	Nishitera machi, koen ji	H-6		977	4	31.4	45	37.3	0.2-1.9	2.1	0.987	1.018
NUE	Hiroshima Castle, honmaru	H-8		1000	4	30.8	45	37.7	0.2-1.9	2.1	0.986	1.015
NUE	Hiroshima Castle, honmaru	H-8'		1000	4	30.8	45	37.7	0.2-1.9	2.1	0.986	1.015
NUE	Hiroshima Castle, honmaru	H-8"		1000	4	30.8	45	37.7	0.2-1.9	2.1	0.986	1.015
JNIRS	City Hall			988	3	31.1	72.4	35.3	1-2	2	0.847	0.873
NUE	Nishitera machi, Shozen ji	H-7		1017	4	30.4	45	37.9	0.2-1.9	2.1	0.986	1.014
JNIRS	Hiroshima University Radioisotope Facility			1470	4	22.1	NA (horizontal surf)	67.9	0.5-1.5	2	0.808	0.814
JNIRS	Hiroshima University Radioisotope Facility			1475	4	22.0	NA (horizontal surf)	68.0	0.5-1.5	2	0.807	0.813
JNIRS	Hiroshima University Radioisotope Facility			1477	4	22.0	NA (horizontal surf)	68.0	0.5-1.5	2	0.807	0.813
JNIRS	Red Cross Hospital			1501	20	21.1	56.5	38.9	0.5-1.5	2	0.895	0.901
JNIRS	Red Cross Hospital			1501	20	21.1	56.5	38.9	0.5-1.5	2	0.895	0.901
JNIRS	Red Cross Hospital			1501	20	21.1	56.5	38.9	0.5-1.5	2	0.895	0.901
JNIRS	Red Cross Hospital			1501	20	21.1	56.5	38.9	0.5-1.5	2	0.895	0.901
JNIRS	Red Cross Hospital			1501	20	21.1	56.5	38.9	0.5-1.5	2	0.895	0.901
NUE	Postal Savings (Chokin Kyoku)	A		1596	19	20.0	NA (horizontal surf)	70.0	0.2-1.9	2	0.900	0.904

Table 5. Continued

Lab	Place name	Sample ID#	RERF list No.	DS02 GR (m)	DS02 ht (m)	Elevation angle (deg)	Azimuthal angle (deg)	Angle of incidence (deg)	Meas. depth (cm)	Density (g/cm^3)	TF, no bldg gamma	TF with bldg gamma
NUE	Postal Savings (Chokin Kyoku)	B		1607	22	19.8	61.5	57.9	0.2-2.1	2	0.971	0.975
NUE	Postal Savings (Chokin Kyoku)	D		1619	19	19.7	NA (horizontal surf)	70.3	0.2-1.9	2	0.897	0.901
NUE	Postal Savings (Chokin Kyoku)	E		1637	19	19.5	NA (horizontal surf)	70.5	0.2-1.9	2	0.895	0.899
NUE	JEMIC	HP7		1788	14.5	18.1	69	27.5	0.2-0.5	2	1.000	1.002
NUE	Myosen-ji "oni-gawara" top	Me-1		1915	7	17.2	16.8	74.0	0.2-1.6	2	0.808	0.809
NUE	Myosen-ji "oni-gawara" bottom	Me-2		1915	7	17.2	16.8	74.0	0.2-1.6	2	0.808	0.809
NUE	Myosen-ji "oni-gawara" top	A-1		1915	7	17.2	16.8	74.0	0.2-1.6	2	0.808	0.809
NUE	Myosen-ji "oni-gawara" bottom	A-2		1915	7	17.2	16.8	74.0	0.2-1.6	2	0.808	0.809
NUE	Hiramoto "oni-gawara" bottom	Hr-1		2067	4.8	16.1	47	45.3	0.2-1.4	2	0.807	0.808
NUE	Hiramoto "Oni-gawara"	B		2067	4.8	16.1	47	45.3	0.2-1.4	2	0.807	0.808
NUE	Hiramoto Oni-gawara	A1-1		2067	4.8	16.1	47	45.3	0.2-1.4	2	0.807	0.808
NUE	Hiramoto Oni-gawara	A1-2		2067	4.8	16.1	47	45.3	0.2-1.4	2	0.807	0.808
NUE	Hiramoto Oni-gawara	A1-3		2067	4.8	16.1	47	45.3	0.2-1.4	2	0.807	0.808
NUE	Hiramoto Oni-gawara	A2		2067	4.8	16.1	47	45.3	0.2-1.4	2	0.807	0.808
NUE	Hiramoto Oni-gawara	A3		2067	4.8	16.1	47	45.3	0.2-1.4	2	0.807	0.808
NUE	Hiramoto Oni-gawara	A4-1		2067	4.8	16.1	47	45.3	0.2-1.4	2	0.807	0.808
NUE	Hiramoto Oni-gawara	A4-2		2067	4.8	16.1	47	45.3	0.2-1.4	2	0.807	0.808
NUE	Hiramoto Oni-gawara	A5		2067	4.8	16.1	47	45.3	0.2-1.4	2	0.807	0.808

Note: Based on the correct location for Shoujunji in Togiya cho, the temple name and cho given by Yamada's RERF memo in 1981. Examination of post-bombing aerial photographs and new city maps indicates there was not a temple at the location of the symbol near (744.44, 1261.72) on the U.S. Army map, the coordinates originally given (without cho or site name) in ABCC TR 6-67. The only other temple in this general area appears to be Senshouji at (26.857, -178.558) on the newer Japanese city map, ground distance = 212 m.

Next Page